A LASER-WIRE SYSTEM AT THE ATF EXTRACTION LINE*

S. T Boogert#, G. Blair, G. Boorman, A. Bosco, L. Deacon, C. Driouichi †, P. Karataev, John
Adams Institute at RHUL, London, UK,
T. Kamps, BESSY, Germany.
N. Delerue, S. Dixit, B. Foster, F. Gannaway, D. F. Howell, M. Qureshi, A. Reichold, R.
Senanayake, John Adams Institute at Oxford, UK.
A. Aryshev, H. Hayano, K. Kubo, N. Terunuma, J. Urakawa, KEK, Ibaraki, Japan.
L. J. Jenner, Liverpool University, Cockcroft Institute, Daresbury Laboratory, Warrington, U.K.
A. Brachmann, J. Frisch, M. Ross SLAC, Stanford, California, U.S.**A.**

Abstract

A new laser-wire (LW) system has been installed at the ATF extraction line at KEK, Tsukuba. The system aims at a micron-scale laser spot size and employs a mode-locked laser system. The purpose-built interaction chamber, light delivery optics, and lens systems are described, and the first results are presented.

INTRODUCTION

The International Linear Collider (ILC) will require a large number of non-invasive beam size measurements to extract the phase space of the electron and positron beams before focusing at the collision point. The large charge and energy densities ~1×10^{10} electrons per bunch at 250 GeV and ~ 1µm vertical beam size of the ILC beams preclude the use of traditional beam size diagnostics, such as wire scanners and screens. These problems are solved by using a high power focused laser beam, the LW, instead of a conventional solid wire

Different technologies may be used in different sub-systems of the ILC. In the ATF damping rings, a system based on a precise optical cavity has been used to good effect [1] and an alternative approach based on a high-power pulsed laser is being pursued at PETRA [2]. For the ILC beam delivery system, the single-shot nature of the electron beam requires the use of high-power pulsed lasers, which is the approach adopted here; the first such device was commissioned at the SLC [3].

In the LW, the laser photons are Compton scattered with electrons from the beam, the total rate of Compton scatters is proportional to the spatial overlap between the laser photon density and electron beam density and given by [4]

$$N_\gamma = N_b \frac{P_L \sigma_C \lambda}{c^2 h} \frac{1}{\sqrt{2\pi}\sigma_s} \exp\left(-\frac{\Delta y}{2\sigma_s^2}\right) \qquad (1)$$

where N_b is the electron bunch population, P_L is the instantaneous laser power, λ is the laser wavelength Δy is the vertical offset between the centres of the laser and electron beams and $\sigma_s^2 = \sigma_l^2 + \sigma_e^2$ is the quadratic sum of electron and laser Gaussian widths. By measuring the Compton rate (N_γ) as a function of relative displacement Δy, the σ_s can be determined. Provided the laser beam size is known precisely, the electron beam size can be extracted in principle. In practice, however, additional machine-related errors may dominate [5]; one of the purposes of a LW experiment at ATF/ATF2 [6] is to quantify and control all the various sources of error that will contribute to an emittance measurement at the ILC.

EXPERIMENTAL CONDITIONS

Accelerator Test Facility

The Accelerator test facility (ATF) is a test accelerator primarily for damping ring development, but also development of new beam diagnostic devices intended for the ILC. The main important parameters of the ATF are given in Table 1.

Beam energy (GeV)	1.28
Num e- per bunch	1×10^{10}
Bunch frequency (Hz)	1.56
Bunch length (ps)	30
Vertical emittance ε_y (m rad)	5×10^{-11}
Vertical emittance ε_y (m rad)	1.6×10^{-9}

Table 1: ATF Parameters

The main components of the ATF are a RF photocathode gun, X-band linac, damping ring and extraction line to a dump. The experimental set up described here is installed after the damping ring extraction system, in the extraction line. A specific electron beam optics has been developed to provide a small vertical beam size at the LW interaction point (IP), with zero vertical and horizontal dispersion. The calculated beam sizes are σ_y = 1µm and σ_x = 20.3 µm. The measured beam size using a wire scanner at the focus location was σ_x = (19.31± 0.72) µm and σ_y = (2.6± 0.3)

---

*Work supported in part by the PPARC LC-ABD Collaboration, the Royal Society, the Daiwa Foundation, and by the Commission of European Communities under the 6th Framework Programme Structuring the European Research Area, contract number RIDS-011899

s.boogert@rhul.ac.uk.

† Now at Niels Bohr Institute, Copenhagen.

μm (the vertical size is consistent with a 1μm electron beam interacting with a 10μm tungsten filament).

Laser and Optical System

The laser consists of four main components; passive mode locked seed laser, Pockels cell pulse picker, regenerative amplifier (RGA), linear amplifier and finally second harmonic generation. The Nd:VAN seed laser produces a pulse train of 20ps long infra red (IR) laser (1064 nm) pulses at a frequency of 357 MHz, which is frequency locked to the ATF RF system. Individual pulses from the seed are selected at the ATF bunch frequency by two Pockels cells and then amplified to 20 mJ and stretched with an etalon to 200 ps in the Nd:YAG RGA. Finally the pulses are amplified in a single pass in two quad-flashlamp pumped Nd:YAG rods to a maximum pulse energy of 1J. Green light is produced using a KD*P crystal and separated from the IR using a dichroic mirror, with a maximum efficiency of 50%. The main parameters of the laser system are in Table 2.

Wavelength (nm)	532
Pulse energy (mJ)	1×10^{10}
Pulse length (ps)	150

Table 2: LW laser parameters

The laser pulses are initially attenuated by 75% using beam splitters before transported down to the ATF extraction line IP.

Accelerator Test Facility

A schematic overview of the LW IP region is shown in Figure 1.

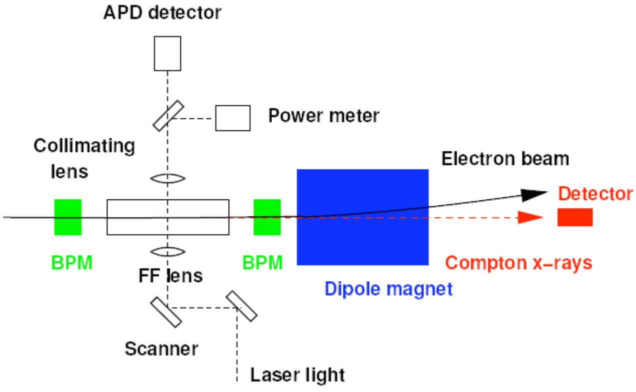

Figure 1: Schematic of the LW IP region.

The laser pulses are transported to the IP via a 3×4 m optical table, used for diagnostics, to a small optical system around the interaction region. The optical layout around the IP is also shown in Figure 1 and a photograph of the chamber, before the associated optics was installed, is shown in Figure 2.

The parallel laser beam is steered onto a scanner, which is a normal optical mount with tilt adjustment in both axes. Then the beam is focused by a singlet lens of nominal focal length f = 150mm (f = 148:8mm for λ = 532nm) to 15μm at the IP. After the IP the diverging laser beam is re-collimated with another singlet lens of focal length f = 100mm (f = 111.8mmf for λ =532nm) and its power measured. A small fraction of the laser pulse that is transmitted through an anti-reflection coated mirror can be measured by an avalanche photodiode detector (APD), which is used to measure the laser light arrival time.

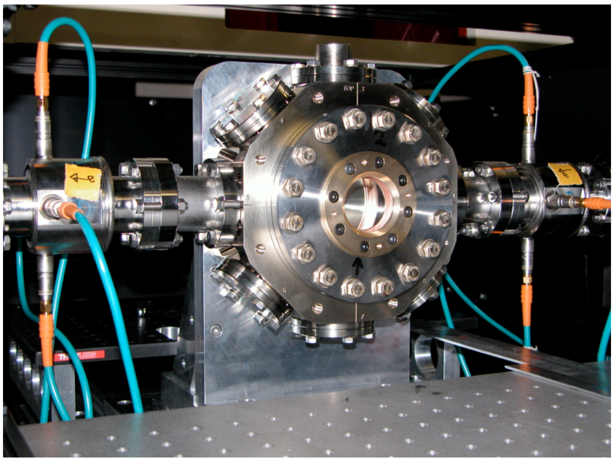

Figure 2: Photograph of the vacuum chamber after installation and before the associated optics was installed.

The electron beam also passes through the chamber. The electron beam position is measured by two strip-line BPMs either side of the LW chamber. One of the horizontal BPM pickups is used to provide a timing signal for the electron beam arrival. Once the laser and electron beams are spatially and temporally in overlap, Compton photons are produced and travel in the electron beam direction. The charged beam is bent into the rest of the extraction line by a dipole and the neutral (photon) signal detected downstream in a gamma-ray detector.

Given the laser and electron parameters above, the maximum Compton scattered photon energy is 28.6 MeV. For a laser beam size of 15 μm, the expected number of Compton photons (from Eq.1) is 51.4 $\times10^3$.

Timing and Spatial Alignment

Given the small electron and laser beam sizes and the short bunch lengths, a dedicated system was used to obtain vertical and temporal overlap between the two transversely colliding beams. A gold-coated silicon knife edge, mounted on a vertical vacuum actuator, was inserted into the chamber at 45° to both the electron and laser beams. The screen was moved so that radiation from the screen (which consists of reflected synchrotron radiation, optical transition, or diffraction radiation) was produced and measured with the APD. The laser (heavily attenuated) is then scanned such as to pass just below the screen, so that the electron and laser beam arrival times were measured on the same detector with common systematic errors (cable lengths, scope resolution). The timing of the mode locked seed laser was then adjusted via altering the phase of 357 MHz reference clock. This procedure guarantees good temporal and vertical overlap of the two beams.

Compton Detector

The high-energy photons generated from the LW Compton events exit the beam pipe via a 1mm thick aluminium window. Approximately 15% of the photons are converted to electron positron pairs in a 4mm thick lead plate on the front of an aerogel Cherekov detector, placed 10 m downstream of the IP. The aerogel is 5cm thick with a refractive index of 1.015, giving a Cherenkov threshold of 2.983 MeV. The Cherenkov photons are detected with a photomultiplier tube and the signal pulse digitized by a gated integrating ADC.

RESULTS AND ANALYSIS

After collision between the electron beam and laser beam, the signal is maximised by adjusting the the laser waist position vertically (y) and horizontally (x) and the timing of the laser system. In order to make a beam size measurement the laser is scanned vertically across electron beam. An example of a vertical waist scan is shown in Figure 3.

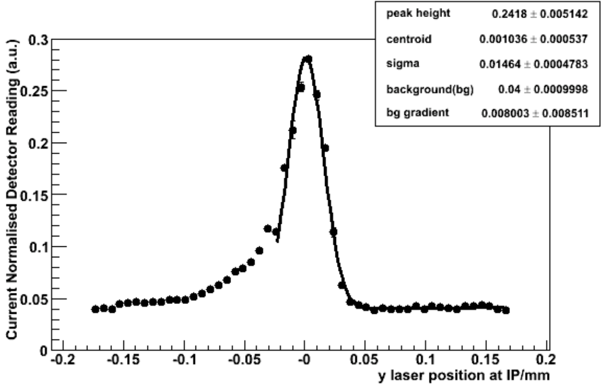

Figure 3: Example of a vertical scan with the ATF extraction line LW system.

The laser waist position is moved vertically and at each position the Compton signal is measured for 20 machine cycles and averaged. The average beam charge is also measured and used to normalise the Compton signal to remove variation due to bunch charge variation from the ATF. The signal as a function of laser position at the IP is approximately Gaussian with a width of (15.2 ± 0.1) μm. There is a clear asymmetry in the signal, which can be attributed either to the transverse profile of the laser pulse or to possible aberrations in the lens such as coma. The current lens is not expected to provide a laser focus sufficiently small to measure the electron beam size as described above. The width of the measured signal is expected to be dominated by the width of the laser beam.

The waist position of the laser pulse is optimised by moving the lens along the laser beam direction. The laser beam was moved to several different positions and a vertical laser scan performed. The size of the extracted Gaussian is plotted as a function of the lens position in Figure 4, from which both the laser beam M^2 and waist beam size can be extracted; the measured M^2 of the laser is 10.6 and the laser waist is 15.4μm. These results are reasonably consistent with measurements performed earlier on the lens with a continuous wave laser.

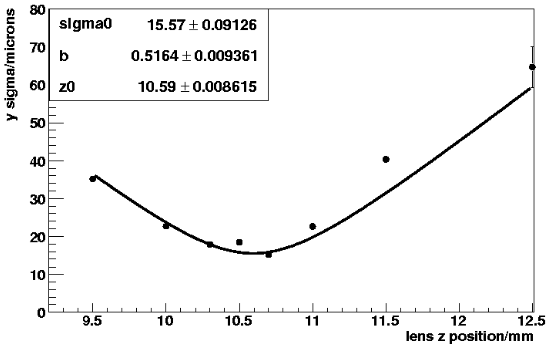

Figure 4: Scan of the laser-waist position by stepping the final focus lens along the laser-beam direction.

CONCLUSIONS AND OUTLOOK

The ATF extraction-line LW has seen first collisions between the 30 ps ATF beam pulses of 1.28 GeV electrons and 150ps, 532nm laser pulses. The results are consistent with a fine electron beam being scanned by a large laser beam; this situation will reverse once the technology has developed, as discussed below.

The size of quadrature beam size, σ_S, measured at the laser beam waist was 15.3 μm and is consistent with optical measurements of the lens before installation in the ATF.

The aim of the ATF system is to verify that beam size measurements of ~1μm electron beams can be performed in the ILC BDS. The first step in this programme has been achieved; the next step is to improve the resolution of the system by improving the transverse mode quality of the laser and upgrading from the commercial lens to a custom-built system with f/2 optics. Longer term, an f/1 system will be designed and it may also be necessary to investigate the use shorter wavelength light.

ACKNOWLEDGEMENTS

We are very grateful to the ATF crew for providing good operating conditions and for their help in setting up the LW system.

REFERENCES

[1] Y.Honda *et al.*Nucl.Instrum.Meth.**A538:**100-115,2005
[2] M. Price *et al.*, these proceedings: TUPCH050.
[3] R. Alley et al. Nucl.Instrum.Meth.**A379**:363-365,1996
[4] P. Tenenbaum and T. Shintake, Ann. Rev .Nucl. Part. Sci. 49:125-162,1999.
[5] G.A. Blair *et al.*, these proceedings: TUPCH048.
[6] ATF2 Proposal KEK Report 2005-2.